Methods in Ecology and Evolution | BRITISH ECOLOGICAL SOCIETY

A spatial point process model to estimate individual centres of activity from passive acoustic telemetry data

Megan V. Winton[1] [iD] | Jeff Kneebone[2] | Douglas R. Zemeckis[3] | Gavin Fay[1]

[1]Department of Fisheries Oceanography, School for Marine Science and Technology, University of Massachusetts, New Bedford, Massachusetts

[2]Anderson Cabot Center for Ocean Life, New England Aquarium, Central Wharf, Boston, Massachusetts

[3]Department of Agriculture and Natural Resources, New Jersey Agricultural Experiment Station, Rutgers, The State University of New Jersey, Toms River, New Jersey

Correspondence
Megan V. Winton
Email: megan.winton@gmail.com

Abstract

1. Failure to account for time-varying detection ranges when inferring space use of marine species from passive acoustic telemetry data can bias estimates and result in erroneous biological conclusions. This potential source of bias is widely acknowledged but often ignored in practice due to a lack of available statistical methods.

2. Here, we describe and apply a spatial point process model for estimating individual centres of activity (COAs) from acoustic telemetry data that can be modified to account for both receiver- and time-specific detection probabilities. We use simulation testing to evaluate the suitability of the proposed models for estimating COAs and compare their performance to that of the popular mean-weighted COA method for a variety of scenarios. We illustrate how the approach can be applied to correct for variable detection ranges by integrating data from moored test tags and demonstrate how accounting for time-varying detection probabilities can impact space use estimates by fitting the model to data collected from a black sea bass (*Centropristis striata*) on a receiver array off the east coast of the United States.

3. The proposed model reduced bias in COA estimates, particularly when tagged individuals occurred along the periphery of the receiver array. The test tag-integrated model largely corrected the bias associated with receiver- and time-specific detection probabilities. When applied to the black sea bass detection data, the model revealed fine-scale movements not apparent when detection ranges were assumed constant.

4. Spatial management practices for coastal marine species are often based on trends in space use inferred from passive acoustic telemetry data, which can be misinterpreted when factors influencing detection ranges are not accounted for. Our approach provides a general framework for estimating individual COAs that can be modified on a study-specific basis to ensure resulting patterns of space use reflect a species' movements and behaviour, rather than variation in receiver detection ranges.

KEYWORDS

acoustic transmitter, centre of activity, detection range, latent spatial process, observation network, passive acoustic telemetry, tag-integrated model

1 | INTRODUCTION

Passive acoustic telemetry is one of the most popular tools for monitoring the occurrence and movements of marine species in coastal environments (Hussey et al., 2017; Kessel et al., 2014). The technology consists of two components: (a) battery-powered acoustic tags, which are programmed to transmit signals at given time intervals, and (b) one or more omnidirectional acoustic receivers that detect, record, and archive tag transmissions. Acoustic transmitters have several advantages compared to other electronic tag types. They are more cost efficient, do not require direct retrieval (as is the case with archival tags), and offer a much longer battery life (up to 10 years for some models). However, their major disadvantage is that they do not provide a continuous time series of locations; tag transmissions are only recorded when a tagged animal is within the detection range of an acoustic receiver. Even when a transmitter is within range, the probability that transmissions are detected declines with distance from the receiver due to signal attenuation, which can vary with substrate type, receiver placement relative to tidal currents or obstructions, biofouling, acoustic reverberation, and environmental conditions (Farmer, Ault, Smith, & Franklin, 2013; Huveneers et al., 2016; Kessel et al., 2014; Simpfendorfer, Heupel, & Collins, 2008). Thus, estimates of tagged animals' space use must be reconstructed from incomplete detection histories, which are biased by both the design of the receiver array and the detection process.

Locations of tagged individuals are commonly inferred using the mean-weighted centre of activity (COA; Simpfendorfer, Heupel, & Hueter, 2002) approach, which is based on the distance-related decay in detection probabilities (i.e. an acoustic receiver close to a tag will log more transmissions than one farther away). Assuming detection probability is a linear function of distance, a tagged animal's COA (here defined as the centroid of space an individual occupied during the time period of interest) is estimated as the mean of receiver locations weighted by the number of detections at each receiver (Simpfendorfer et al., 2002). In most situations, detection probability declines nonlinearly with distance and varies with environmental conditions even among receivers in a single array (Farmer et al., 2013; Huveneers et al., 2016). Variation in receiver-specific detection probabilities can result in biased estimates of movement and space use if not accounted for during estimation (Pedersen & Weng, 2013). However, the mean-weighted COA approach is not mechanistic (as is also the case for alternative nonparametric regression models inspired by it; Hedger et al., 2008), and cannot be directly modified to account for time-varying detection probabilities, even if important covariates are identified via range tests using stationary reference tags (e.g. Huveneers et al., 2016).

Here, we develop a spatial point process (SPP) model to estimate individual COAs from passive acoustic telemetry data. The approach models both the spatial distribution of individual animals and the observation process underlying recorded detection histories, making it well suited for addressing bias associated with the detection process. Models of this type are often used for the analogous issue of imperfect detection when inferring species distributions from georeferenced occupancy and mark-recapture datasets (Royle, Chandler, Sollmann, & Gardner, 2014; Royle & Dorazio, 2008). We conduct simulations to investigate the suitability of SPP models for estimating COAs from acoustic telemetry data and compare their performance to that of the popular mean-weighted method. To illustrate how the approach can be used to correct for receiver-specific variation in detection probabilities, we extend the SPP model to incorporate detection data collected from a moored, known-location tag. Finally, we demonstrate how accounting for time-varying detection probabilities can affect estimates of space use by fitting the model to acoustic detection data from a black sea bass (*Centropristis striata*) collected on a receiver array off the east coast of the United States.

2 | MATERIALS AND METHODS

2.1 | Model background

Conceptually, we consider acoustic detections as the realization of a continuous latent spatial process (here the distribution of individuals in space; Aarts, Fieberg, & Matthiopoulos, 2012) that are biased as the result of the observation process (i.e. the location and detection range of individual receivers). A detection indicates an individual was within the detection range of a given receiver but does not provide information on the individual's location within that range. The distribution of individual COAs is not directly observed, so we model it as a latent spatial effect (Royle et al., 2014).

Assuming no prior information is available to inform the distribution of COAs over the study area, S, we represent locations of individual COAs i at each time step t, c_{it}, as the realization of a binomial SPP (Royle et al., 2014), where the number of tagged individuals at each time step is known and COA locations are assigned a uniform prior distribution over space:

$$c_{it} \sim \text{Uniform}(S) \tag{1}$$

The resulting point pattern is informed by the available detection data and will result in nonuniform distributions if, for example, tagged individuals aggregate in parts of the monitored area.

Acoustic receivers operate continuously, but acoustic tags transmit at a programmed nominal delay (typically every 1–2 min) to conserve battery life and avoid conflicts between transmissions from multiple tags (Heupel, Semmens, & Hobday, 2006). Given the maximum expected number of transmissions K_t over a given time interval, we model the number of observed detections as a binomial random variable:

$$y_{ijt} \sim \text{Binomial}(K_t, p_{ijt}), \tag{2}$$

where p_{ijt} is the detection probability for individual i at receiver j at time step t. Alternatively, the number of detections could be modeled as Poisson, which may be preferable if transmission intervals are programmed to vary over time, or if the intent is to model space use of individuals tagged with different transmitter types.

Detection probability is modelled as a function of the distance between a receiver and the individual's COA at each time step, which can be represented by any plausible decreasing function of distance. Here we use a Gaussian decay function (Royle et al., 2014):

$$p_{ijt} = p_0 \exp\left(-\frac{1}{2\sigma^2}||\mathbf{x}_j - \mathbf{c}_{it}||^2\right), \qquad (3)$$

where p_0 is the detection probability at a distance of zero (here assumed equal for all receivers); σ^2 is the variance of the Gaussian decay function; and $||\mathbf{x}_j - \mathbf{c}_{it}||$ is the Euclidean distance between the location of receiver j and c_{it}. Here p_{ijt} is proportional to a Gaussian kernel, implying a bivariate normal model of space use (commonly assumed when estimating home ranges of tagged individuals; Calenge, 2006).

The model for detection probabilities can be extended to account for effects of environmental covariates, and individual-, receiver-, or time-specific differences:

$$\text{logit}(p_{0ijt}) = \beta_0 + \beta\mathbf{X}_{ijt} \qquad (4)$$

$$p_{ijt} = p_{0ijt} \exp\left(-\frac{1}{2\sigma^2}||\mathbf{x}_j - \mathbf{c}_{it}||^2\right), \qquad (5)$$

where β_0 is an intercept term, β represents a vector of regression coefficients, and $\mathbf{X}$ is a vector of covariates specific to an individual, receiver, or time interval. Here, covariates scale the zero-distance detection probability rather than the shape of the detection function (Pedersen & Weng, 2013). Variation in space use between individuals or over time can be accounted for by allowing individual- or time-specific estimates of σ_{it}^2 (Royle et al., 2014), though the degree of complexity supported by the dataset available should be considered prior to doing so.

2.2 | Model fitting and parameter estimation

We fit a Bayesian version of the SPP model using the Stan software (Carpenter et al., 2016; Stan Development Team 2017), which implements the No-U-Turn Sampler algorithm (Hoffman & Gelman, 2014) in R (R Core Team 2016). Regression coefficients were assigned Cauchy priors (location = 0, scale = 2.5; Gelman, Jakulin, Pittau, & Su, 2008). For each model fitted, we ran four chains of length 10,000 without thinning, discarding the first half of each chain as "warm-up" (the default in Stan). To diagnose non-convergence and confirm chains had achieved stability, we examined the potential scale reduction value (which should be close to 1) and the effective sample size of the resulting marginal posterior distributions for estimated parameters.

2.3 | Evaluating bias associated with the mean-weighted COA approach

Assuming that detection probability is a linear function of distance under the mean-weighted COA approach can be considered a form of model misspecification when the true relationship

is nonlinear (e.g. Farmer et al., 2013; Huveneers et al., 2016). The mean-weighted method also restricts resulting position estimates to the area within the minimum convex polygon of a receiver array's bounds (Simpfendorfer et al., 2002). Thus, the method cannot take advantage of information provided by time periods when individuals are either not detected or are only detected on the peripheral receivers of an array. For example, if an individual is only detected along the edge of an array during a time interval, its location is likely outside the array (unless the array is bounded by uninhabitable areas). In such situations, position estimates from the mean-weighted COA method will be biased (Simpfendorfer et al., 2002).

We used simulations to test the effect of model misspecification on COA estimates by applying both the mean-weighted COA method and the SPP model to data generated from nonlinear detection functions. Using Equation (3), we simulated 1 hr of detection data for 10 individuals on an array of 30 receivers assuming an 82% probability of detection at a distance of 0 (p_0 = 0.82) and σ = 300 m (Supporting Information Figure S1). Receivers were spaced 500 m apart to ensure overlap in detection ranges; this configuration represents a common array design when the objective is to quantify fine-scale movements in an area (Dean, Hoffman, Zemeckis, & Armstrong, 2014). Tags were assumed to have an average nominal delay of 1.5 min, translating to a maximum of K = 40 possible detections logged by an individual on any given receiver during the 60-min time interval. Probability of detection at a given distance was assumed constant among individuals and receivers. True COA locations were randomly generated from two uniform distributions with bounds representing the spatial extent of the receiver array in the east-west and north-south directions plus a 500 m buffer on all sides, which allowed for COAs along the periphery of the array. The mean-weighted COA method cannot estimate positions for individuals with zero detections, so we limited the buffer extent to ensure all individuals would be detected at least once to allow comparison between methods.

We applied the mean-weighted COA and the SPP model to 100 simulated datasets and assessed how well each recovered the COAs generating the observations. For each method, we calculated the root mean squared error (RMSE) of the Euclidean distance between the estimated and true COA locations. For the SPP model, the posterior median was used to calculate error; we also calculated the proportion of the individual 95% credible intervals encompassing the true COAs in each simulation.

2.4 | Ramifications of time interval selection and receiver density

Even if the functional form of the detection probability is specified correctly, the accuracy of the resulting COA estimates will vary with the time interval selected (Simpfendorfer et al., 2002), the design of the receiver array (Pedersen, Burgess, & Weng, 2014), and the noise environment (Simpfendorfer et al., 2008). To evaluate the impact of varying the time interval used for COA estimation, we simulated detection data for 10 tagged individuals at intervals of 5, 15, 30, 60, and 90 min, which spans the lower end of the range typically applied

to estimate short-term COAs (e.g. Freitas, Olsen, Moland, Ciannelli, & Knutsen, 2015; Harasti, Lee, Gallen, Hughes, & Stewart, 2015). To investigate the effect of variable receiver coverage, we simulated 1 hr of detection data for 10 individuals on increasingly sparse receiver arrays. We randomly subset the array of 30 receivers (density of 6 receivers/km^2) to obtain subsets of the original simulated datasets for arrays with 20, 15, 10, and 5 receivers (densities of 4, 3, 2, and 1 receiver/km^2). The detection function and tag transmission interval were specified as for the baseline scenario. The SPP model and mean-weighted COA were applied to each simulated dataset, and the error in the resulting estimates calculated as described above.

2.5 | Accounting for receiver-specific variation in detection probabilities

If time series of relevant environmental drivers are available, detection probabilities can be modeled directly as a function of covariates (Farmer et al., 2013; Huveneers et al., 2016). However, in many cases, such data are not available for the entire monitoring period or for all potentially important covariates. When data from stationary test transmitters are available, variation in detection probabilities can be directly estimated by comparing the expected number of transmissions during a given time interval with those observed. Previous approaches for incorporating test tag data involve scaling the expected number of detections from a transmitter at a given distance based on the observed time series of detections, rather than directly informing p_0 (Pedersen & Weng, 2013). Here we provide an alternative approach, which integrates data from one or more test tags directly into COA estimates via a simple extension of the SPP model described above. The test tag-integrated model includes an additional binomial likelihood component for the observed test tag data that estimates the probability of detection (p_{ijt}) by comparing the number of detections logged by each test tag i at

receiver j during time interval t (l_{ijt}) versus those emitted from the test tag, K_t:

$$l_{ijt} \sim \text{Binomial}(K_t, p_{ijt}), \tag{6}$$

where the test tag's COA (c_{it} in Equation 3) is specified as its known location rather than estimated. The resulting model integrates detections from both tagged individuals and test transmitters when estimating detection probabilities and jointly estimates p_0 and σ simultaneously from both data sources (Maunder & Punt, 2013).

To demonstrate how this model can be applied to correct for variation in detection probabilities among receivers, we fit the test tag-integrated model to detections from a stationary, moored test transmitter (model V9P-2H; Vemco AMIRIX Systems, Inc.). The tag was mounted to a steel beam and deployed in an array of receivers (Vemco model VR2W) as part of a study investigating discard mortality of black sea bass in the U.S. Mid-Atlantic. The transmitter was deployed in the middle of the array (which was centred on a shipwreck located 85 km off the coast of Cape May, New Jersey, in 45–55 m depth; Figure 1) to provide reference for the number of detections expected from a dead fish under varying conditions. For illustrative purposes, we limited our analysis to detection data from the first 153 hr after test tag deployment, during which detection data from a 366 mm tagged black sea bass were also available. The fish was captured via rod-and-reel the same day the test tag was deployed. Capture and handling protocols were approved by IACUC (Rutgers the State University of New Jersey IACUC protocol #15-049). Following tagging and release, the fish remained within the receiver array for 6 days and was eventually recaptured 114 days after tagging. Both tags were programmed to transmit at an average delay of 2 min, with a random delay of ±1 min ($K = 30$).

To evaluate whether integration of the reference tag data was sufficient to account for bias due to varying detection probabilities,
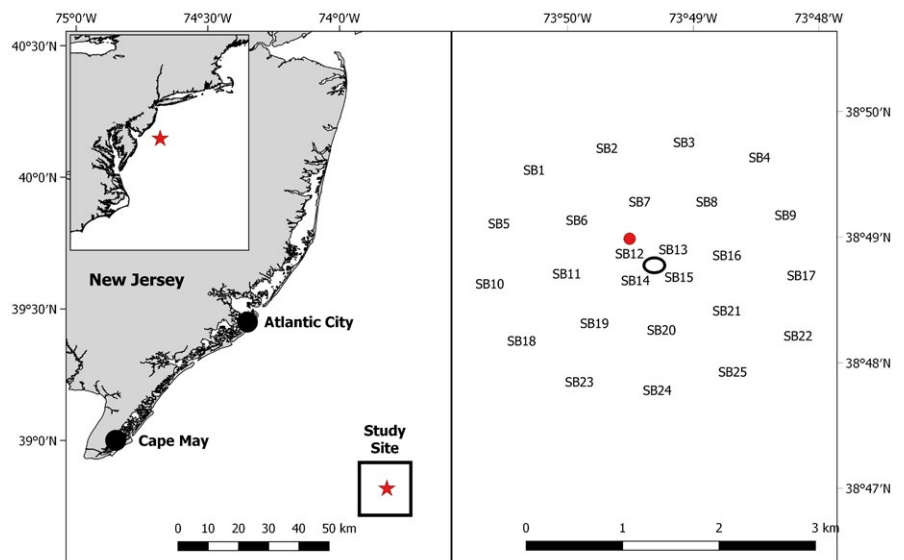
FIGURE 1 Receiver array deployed to monitor discard mortality of black sea bass off New Jersey, USA. Black points indicate receiver locations. The red circle indicates the position of the moored test tag and the open black oval the location of a shipwreck

we compared the results of applying the test tag-integrated model to estimate the test transmitter's location with those produced using the mean-weighted COA and the SPP model assuming constant detection probabilities. For the test tag-integrated approach, we fit the model to detections from the test transmitter but treated it as a tagged individual with unknown location. We then calculated the RMSE in the north-south and east-west coordinate estimates from each method. To demonstrate how accounting for variation in detection probabilities can influence resulting estimates of space use for a tagged individual, we applied the three COA estimation methods to data collected from the tagged black sea bass over the same period.

For comparison, we calculated the distance between estimated COAs at each successive time step as a metric of movement using the R package 'ADEHABITATLT' (Calenge, 2006).
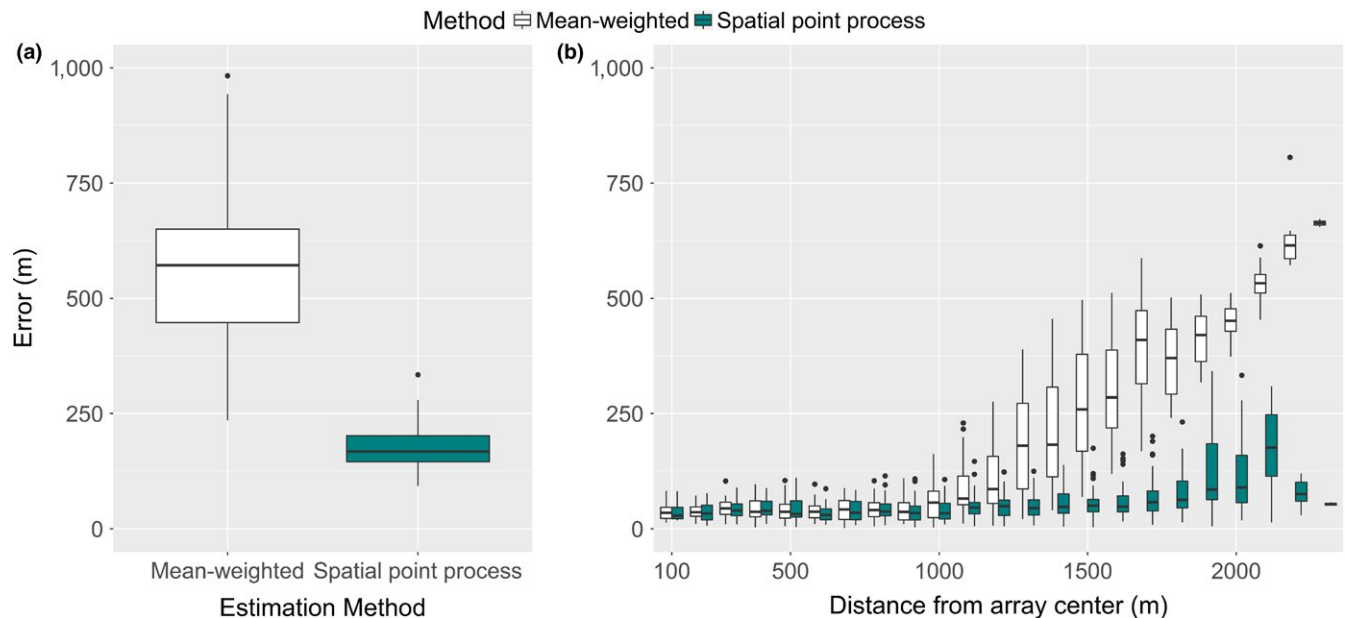
3 | RESULTS

3.1 | Simulation scenarios

Applying the mean-weighted COA approach to detection histories generated as a nonlinear function of distance resulted in substantial error, even when receiver detection ranges overlapped ("baseline"

Simulation scenario	Mean weighted	Spatial point process	Proportion including true COA
Baseline	606 (256–940)	170 (117–299)	0.95 (0.70–1.00)
Time interval			
5 min	729 (501–1,018)	592 (389–850)	0.95 (0.50–1.00)
15 min	666 (340–1,011)	343 (229–491)	0.95 (0.70–1.00)
30 min	641 (319–964)	239 (171–417)	0.94 (0.70–1.00)
60 min*	606 (256–940)	170 (117–299)	0.95 (0.70–1.00)
90 min	608 (258–940)	135 (90–207)	0.94 (0.60–1.00)
Receiver density			
1/km^2	1,305 (703–1,767)	1,043 (360–1,735)	0.92 (0.25–1.00)
2/km^2	1,057 (697–1,561)	677 (216–1,351)	0.93 (0.57–1.00)
3/km^2	942 (645–1,336)	378 (188–1,369)	0.95 (0.71–1.00)
4/km^2	789 (471–1,130)	282 (167–620)	0.95 (0.70–1.00)
6/km^2	606 (256–940)	170 (117–299)	0.95 (0.70–1.00)

TABLE 1 Median root mean squared error (RMSE; in m) of the Euclidean distance between simulated and estimated centres of activity. The 2.5 and 97.5% RMSE from all simulations are indicated in parentheses. Baseline scenario corresponds to a 60-min time interval and a receiver density of 6 receivers/km^2; a * indicates a scenario identical to the baseline. The mean and range of 95% credible intervals encompassing the true centre of activity (across all individuals) for the spatial point process model are also presented

FIGURE 2 Root mean squared error (RMSE; in m) of centre of activity estimates resulting from applying the mean-weighted method and the spatial point process model to 60-min of simulated detection data (a) in aggregate and (b) as a function of an individual's distance from the centre of the receiver array. For the spatial point process model, RMSEs were calculated using the posterior median for each individual in each simulation. Lines within boxes represent the median RMSE across simulations and box extents the first and third quartiles, with whiskers extending 1.5 times the interquartile range from the median
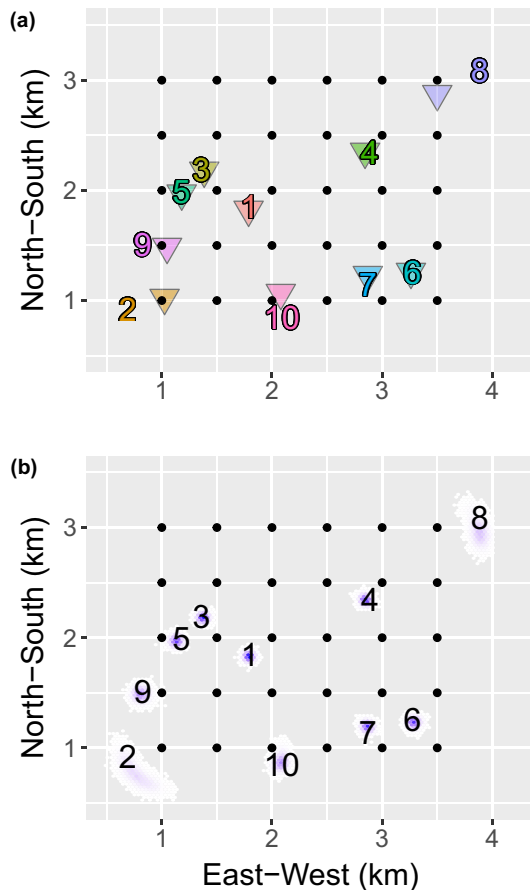
FIGURE 3 Sixty-minute centre of activity estimates from applying (a) the mean-weighted centre of activity algorithm and (b) the spatial point process model to a simulated dataset. Numbers indicate the true centres of activity of ten individuals. Inverted coloured triangles represent position estimates corresponding to the coloured numbers in (a). In (b), the estimate is represented by the posterior distribution of each individual's estimated activity centre, with dark blue areas having highest posterior probability. Black points indicate receiver locations

scenario in Table 1). The SPP model reduced error in COA estimates (Figure 2) and recovered parameter values used to generate simulated datasets (Supporting Information Figure S2). When individual simulations were examined, the SPP model outperformed the mean-weighted approach for individuals with COAs along the periphery of the array (Figure 2; Figure 3 presents an example from one simulation).

For all scenarios, credible interval coverage for the SPP model was high, though uncertainty increased at lower receiver densities and at shorter time intervals (Supporting Information Figure S2). Over short time intervals (<30 min) and at low receiver densities (<4 receivers/km^2), estimates of p_0 were not well defined (Supporting Information Figure S2); however, errors in the COA estimates were still lower than the mean-weighted method (Figure 4). The credible intervals for individual COAs encompassed the true COA near the nominal 95% rate in most simulations (Table 1) and reflected the uncertainty associated with each detection history (i.e. COA estimates

for individuals with fewer detections were more uncertain; Figure 3). While performance of the SPP model improved with longer time intervals, the error from the mean-weighted approach was relatively constant (Table 1; Figure 4a). As expected, the error resulting from applying both methods decreased as the density of receivers increased (Figure 4b).

3.2 | Accounting for receiver-specific variation in detection probabilities

The number of detections logged at each receiver within range of the moored test tag over the 153-hr period varied substantially (in particular SB6, SB7 and SB11; Supporting Information Figure S3), though receivers farther from the tag generally logged fewer detections. When receiver-specific variation was ignored, both the mean-weighted COA and SPP approaches produced biased hourly location estimates; the error from fitting the SPP model assuming constant detection probabilities was greater in the north-south direction (Figure 5). The tag-integrated SPP model allowing for receiver- and time-specific detection probabilities largely corrected the bias in test tag location estimates (Figure 5) and reflected increased uncertainty in the estimate for time intervals with fewer detections (Supporting Information Figure S4). Lingering northward bias appeared to be due to high numbers of detections logged by a receiver at 499 m (receiver SB7) relative to the number of detections logged by those closer to the tag at 200 and 474 m (SB12 and SB13; Figure 1, Supporting Information Figure S3). Compared to the SPP model assuming constant detection probabilities, which estimated p_0 at 0.69, receiver- and time-specific parameter estimates from the tag-integrated model reflected the observed variation (Supporting Information Table S1; Figures S3 and S4).

During the 153-hr period examined, the tagged black sea bass was detected 3,002 times on 9 receivers (Supporting Information Table S2). When applied to the fish's hourly detection data, both the mean-weighted and SPP assuming constant detection probabilities produced relatively static hourly COA estimates (Figure 6 presents the first 10 hr for illustration). The test tag-integrated model shifted COA estimates according to observed variation in detection probabilities (Supporting Information Table S1) and reflected patterns of nondetection as well as detection (Figure 6). For example, the fish was detected most often on four central receivers that also detected the test tag (SB12, SB13, SB14 and SB15), but was never detected by receivers SB6 and SB7. For time periods in which SB6 and SB7 had large detection radii (Supporting Information Table S1; Figure S3), COA estimates were shifted slightly to the south of the detecting receivers to reflect nondetection by these neighbouring receivers with high detection probabilities (e.g. hours 1 and 2). Detection probabilities at a given receiver varied substantially over time (Supporting Information Table S1; Figure S3), which influenced the resulting COA estimates. For example, in hours 3 and 4, the detection radii of receivers SB6 and SB15 dropped, subsequently shifting the estimated COA to the southwest and east, respectively (Figure 6). COA estimates for hours in which few detections were logged (e.g. hours 3
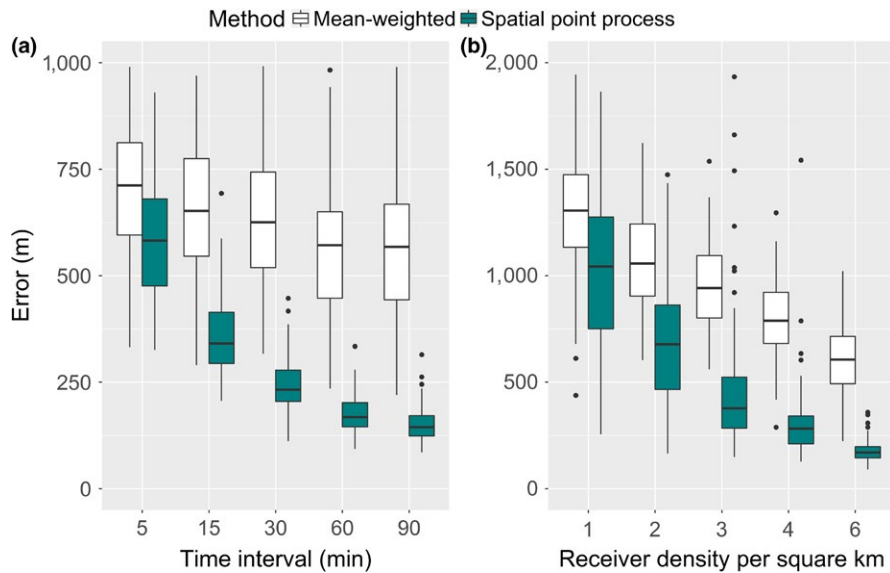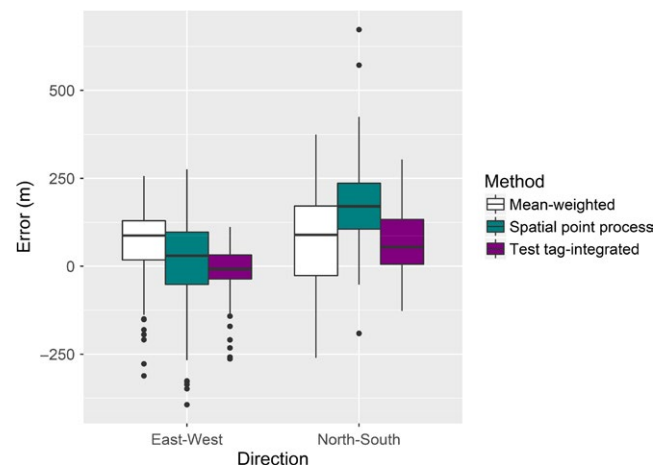
FIGURE 4 Root mean squared error (RMSE; in m) in the centre of activity estimates resulting from applying the mean-weighted centre of activity algorithm and the spatial point process model to simulated detection data (a) over time intervals from 5 to 90 min and (b) varying receiver densities on a 60-min time step. Lines in boxes represent the median RMSE and box extents the first and third quartile, with whiskers extending 1.5 times the interquartile range from the median

and 6) had a wider posterior distribution with more uncertainty in the probable location (Supporting Information Table S2; Figure 6). While COA estimates from all three methods were similar during some time periods (e.g. hours 5, 7, 8 and 9), the test tag-integrated model revealed a larger degree of apparent movement than the mean-weighted approach and the SPP model not accounting for variation in detection probabilities (Table 2; Figure 6).

4 | DISCUSSION

The need to account for variable detection ranges when inferring space use from passive acoustic telemetry data has been often cited (Kessel et al., 2014) but more often ignored in practice due to a lack of available statistical frameworks. Here we described and applied a hierarchical SPP model for estimating individual COAs that can be modified to account for variation in receiver-specific detection probabilities over time. Our method for modelling the detection function is similar to the state-space modelling approach proposed to account for time-varying detection probabilities by Pedersen and Weng (2013), which was subsequently reformulated in a Bayesian framework by Alós, Palmer, Balle, and Arlinghaus (2016). However, our formulation does not prespecify a movement model, estimates COA locations in continuous rather than discrete space, and directly integrates stationary test tag data into COA estimates for tagged individuals. As presented here, our approach does not account for temporal correlation in the data but does provide a general basis for estimating individual COAs (as well as their uncertainty) that can be readily incorporated into a variety of movement or space use models depending on specific application needs.

Our simulation scenarios suggested COA estimates are sensitive to model misspecification, even when detection ranges of individual receivers overlap. In all scenarios, errors from the mean-weighted COA method were higher than for the SPP model. Higher errors associated with the mean-weighted approach can

FIGURE 5 Root mean squared error (RMSE; in m) in centre of activity estimates in east-west and north-south directions from applying the mean-weighted centre of activity algorithm, spatial point process model assuming constant detection probabilities, and test tag-integrated spatial point process model to detection data collected from a stationary test tag. Lines within boxes represent the median RMSE and the extent of the box the first and third quartile, with whiskers extending 1.5 times the interquartile range from the median

be partially attributed to simulated individuals with COAs outside the bounds of the array. If we had assumed the array was bounded by uninhabitable regions the error resulting from the mean-weighted method may have been lower. However, in most applications, receiver arrays do not directly abut areas that cannot be occupied to ensure receivers function continuously (e.g. remain submerged at lowest tide; Kneebone, Chisholm, & Skomal, 2012) and tag transmissions are not reflected or blocked by obstacles (Pedersen et al., 2014). As our simulations showed, in instances where individuals remain in the area but are not constrained to array bounds, the SPP model will outperform the mean-weighted approach. For mobile species that may leave and
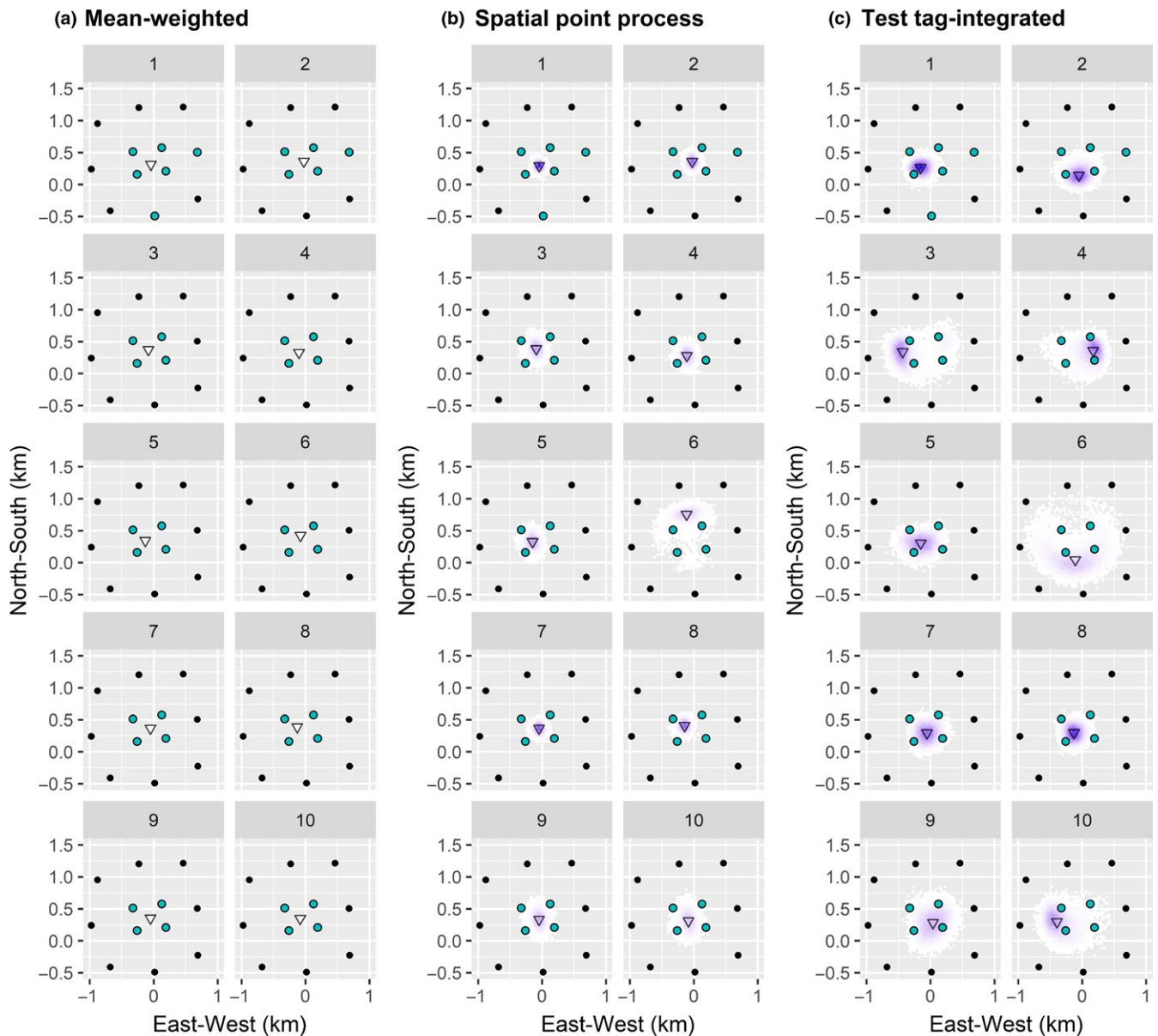
FIGURE 6 Sequential 60-min centre of activity estimates (inverted triangles) for 10 hr of detection data from a tagged black sea bass from applying the (a) mean-weighted centre of activity algorithm, (b) a spatial point process model assuming constant detection probabilities, and (c) the test tag-integrated spatial point process model accounting for receiver- and time-specific detection probabilities. The posterior distributions for both applications of the spatial point process model are presented. Points indicate the location of detecting (aquamarine) and nondetecting (black) receivers in each hour

re-enter the array between time steps, the SPP models presented here could be extended to explicitly account for such movement (Royle et al., 2014) based on detections logged in other receiver arrays or locations reported by other tag types (Braun, Skomal, Thorrold, & Berumen, 2015).

Model performance changed with the time interval selected for estimation as well as with receiver array density, highlighting important considerations when designing acoustic telemetry studies. For the simulated array, errors from the mean-weighted COA approach were relatively invariant to the time interval used for estimation at high receiver densities. However, errors associated with the SPP model decreased substantially at longer time intervals; more

accurate position estimates were produced when more detections were available. While aggregating detection data over longer time intervals to improve precision may be reasonable for territorial or resident species, long time intervals can bias estimates of the position of constantly swimming species, such as sharks (Alós et al., 2016). When available, data from moored test tags should be used to determine the appropriate time interval given observed variation in detection probabilities; the time step selected should be sufficiently small so as to reduce error in position estimates due to variation in detection ranges but large enough to allow a sufficient number of detections for estimation (Hedger et al., 2008). The decline in model performance at lower receiver densities was intuitive and consistent

	Distance (m)				
Estimation method	Mean	Median	Minimum	Maximum	*SD*
Mean-weighted	86.5	60.9	0.0	1,172.5	115.1
Spatial point process model	227.5	104.3	6.6	1,842.5	332.5
Test tag-integrated model	329.5	258.9	11.2	2,128.1	333.6

TABLE 2 Euclidean distance (in m) between sequential centre of activity estimates at each time step resulting from applying three estimation methods to 6 days of detection data collected from a tagged black sea bass

with the results of simulations conducted by others (Hedger et al., 2008; Pedersen & Weng, 2013), but our results show that errors can increase substantially with even slight changes in coverage. Conducting simulations such as those presented here prior to receiver deployment could help ensure array designs are sufficient to answer specific questions of interest (Pedersen et al., 2014).

Failure to consider receiver-specific detection probabilities can result in biased COA estimates, even when the SPP model is applied. Depending on the particular receiver array and the degree to which detection probabilities vary among receivers, the SPP model may be more biased than the mean-weighted approach when time-varying detection ranges are not accounted for, as in our application to test tag data. Even when the tag-integrated model was applied to estimate position of the test tag, bias in COA estimates remained. This was likely due to our choice to apply a Gaussian detection function, which implies that detection probabilities decline monotonically with distance and are symmetrical around the receiver's location (i.e. are isotropic). Estimates will be robust to slight model misspecification implied by distance decay functions of similar shape (Fay & Punt, 2013), but in some cases detection probabilities may actually increase over short distances before declining; decreases in detection probabilities in the immediate vicinity of receivers have been documented in the field (i.e. acoustic "shadows" or the "doughnut effect"; Kessel et al., 2015). Similar scenarios can arise when acoustic reverberations are an issue (Claisse et al., 2011). This may have been the case for the black sea bass array, which was centred on a shipwreck. Detection probability may also vary with direction, the tagged animal's orientation to receivers (Pedersen & Weng, 2013), and tag placement (i.e. external or internally implanted transmitters; Dance, Moulton, Furey, & Rooker, 2016). Future studies should seek to evaluate detection functions that account for nonmonotonic declines with distance as well as geometric anisotropy. As part of any application, researchers should conduct a thorough model selection, particularly when mechanistic relationships between detection probabilities and environmental drivers are used.

Our results contribute to the growing body of literature suggesting the need to acknowledge and account for receiver-specific variation in detection probabilities when inferring space use and movements from passive acoustic telemetry data. Our test tag-integrated approach can be used to jointly estimate detection probabilities from detection data collected from both test tags and tagged individuals, even when data on environmental factors affecting detection probabilities are not available. In the black sea bass case study, the test tag-integrated model revealed fine-scale movements not apparent in location estimates from both the mean-weighted COA and the SPP model assuming constant detection probabilities. The ability to more accurately estimate fine-scale movements, particularly along the periphery of an acoustic array, is advantageous when monitoring animal movements within spatially-discrete areas (e.g. marine protected areas; Filous et al., 2017) and for applications when horizontal movements are used to infer animal fate (Kneebone, Chisholm, Bernal, & Skomal, 2013).

One potential downside of the proposed approach relative to the mean-weighted COA is the increased computation time required for model fitting. When applied to the black sea bass data, the SPP model assuming constant detection probabilities took 1.3 hr to run on a laptop computer with a four-core central processing unit. The full, test tag-integrated model (which estimated time- and receiver-varying detection probabilities) took 4.2 hr to run; analysis of longer time series from multiple individuals would take considerably longer. As with any modelling application, computing time scales with model complexity; the degree of complexity required to answer the question at hand should be judiciously considered.

We prefer the Bayesian approach for COA estimation due to its treatment of uncertainty but realize the longer computational time required may be prohibitive for applications using acoustic telemetry to track individuals over long time periods. Future work will investigate the performance of the models presented here when fitted in a maximum likelihood framework, which will reduce run-times. While recent advances in fitting techniques and the uptake of compiled languages in ecology (e.g. Stan, the software used here, and Template Model Builder; Kristensen, Nielsen, Berg, Skaug, & Bell, 2016) have significantly reduced the run-time required to fit a wide range of hierarchical models, some applications may require access to additional computing capacity, as is typically the case when reconstructing tracks from archival satellite tag data (Braun, Galuardi, & Thorrold, 2017). However, the increased computing time seems well-spent given that failure to account for time-varying detection probabilities may result in interpretations that do not accurately reflect a species' biology (Payne, Gillanders, Webber, & Semmens, 2010). Our approach provides a general framework for modelling detection probabilities that can be modified on a study-specific basis to ensure resulting patterns of space use reflect the behaviour of the species being studied, rather than variation in receiver detection ranges.

ACKNOWLEDGEMENTS

AUTHORS' CONTRIBUTIONS

M.V.W. and J.K. conceived the idea; M.V.W. and G.F. designed the analytical approach; J.K. and D.R.Z. designed the field methods and collected the data; M.V.W. and G.F. analyzed the data; M.V.W. led the writing of the manuscript. All authors made important contributions to the draft and approved the final version for publication.

DATA ACCESSIBILITY

Code and datasets required to replicate the black sea bass analysis presented are provided as part of the R package 'TelemetrySpace', which is available via GitHub https://doi.org/10.5281/zenodo.1344613

ORCID

Megan V. Winton 🆔 http://orcid.org/0000-0003-2628-7022

REFERENCES

Aarts, G., Fieberg, J., & Matthiopoulos, J. (2012). Comparative interpretation of count, presence–absence and point methods for species distribution models. *Methods in Ecology and Evolution*, *3*, 177–187. https://doi.org/10.1111/j.2041-210X.2011.00141.x

Alós, J., Palmer, M., Balle, S., & Arlinghaus, R. (2016). Bayesian state-space modelling of conventional acoustic tracking provides accurate descriptors of home range behavior in a small-bodied coastal fish species. *PLoS ONE*, *11*, e0154089. https://doi.org/10.1371/journal.pone.0154089

Braun, C. D., Galuardi, B., & Thorrold, S. R. (2017). HMMoce: An R package for improved geolocation of archival-tagged fishes using a hidden Markov method. *Methods in Ecology and Evolution*, *9*, 1212–1220. https://doi.org/10.1111/2041-210X.12959

Braun, C. D., Skomal, G. B., Thorrold, S. R., & Berumen, M. L. (2015). Movements of the reef manta ray (*Manta alfredi*) in the Red Sea using satellite and acoustic telemetry. *Marine Biology*, *162*, 2351–2362. https://doi.org/10.1007/s00227-015-2760-3

Calenge, C. (2006). The package "adehabitat" for the R software: A tool for the analysis of space and habitat use by animals. *Ecological Modelling*, *197*, 516–519. https://doi.org/10.1016/j.ecolmodel.2006.03.017

Carpenter, B., Gelman, A., Hoffman, M., Lee, D., Goodrich, B., Betancourt, M., … Riddell, A. (2016). Stan: A probabilistic programming language. *Journal of Statistical Software*, *76*, 14005. https://doi.org/10.18637/jss.v076.i01

Claisse, J. T., Clark, T. B., Schumacher, B. D., McTee, S. A., Bushnell, M. E., Callan, C. K., … Parrish, J. D. (2011). Conventional tagging and acoustic telemetry of a small surgeonfish, *Zebrasoma flavescens*, in a structurally complex coral reef environment. *Environmental Biology of Fishes*, *91*, 185–201. https://doi.org/10.1007/s10641-011-9771-9

Dance, M. A., Moulton, D. L., Furey, N. B., & Rooker, J. R. (2016). Does transmitter placement or species affect detection efficiency of tagged animals in biotelemetry research? *Fisheries Research*, *183*, 80–85. https://doi.org/10.1016/j.fishres.2016.05.009

Dean, M. J., Hoffman, W. S., Zemeckis, D. R., & Armstrong, M. P. (2014). Fine-scale diel and gender-based patterns in behaviour of Atlantic cod (*Gadus morhua*) on a spawning ground in the Western Gulf of Maine. *ICES Journal of Marine Science*, *71*, 1474–1489. https://doi.org/10.1093/icesjms/fsu040

Farmer, N. A., Ault, J. S., Smith, S. G., & Franklin, E. C. (2013). Methods for assessment of short-term coral reef fish movements within an acoustic array. *Movement Ecology*, *1*, 7. https://doi.org/10.1186/2051-3933-1-7

Fay, G., & Punt, A. E. (2013). Methods for estimating spatial trends in Steller sea lion pup production using the Kalman filter. *Ecological Applications*, *23*, 1455–1474. https://doi.org/10.1890/12-1645.1

Filous, A., Friedlander, A., Wolfe, B., Stamoulis, K., Scherrer, S., Wong, A., … Sparks, R. (2017). Movement patterns of reef predators in a small isolated marine protected area with implications for resource management. *Marine Biology*, *164*, 2. https://doi.org/10.1007/s00227-016-3043-3

Freitas, C., Olsen, E. M., Moland, E., Ciannelli, L., & Knutsen, H. (2015). Behavioral responses of Atlantic cod to sea temperature changes. *Ecology and Evolution*, *5*, 2070–2083. https://doi.org/10.1002/ece3.1496

Gelman, A., Jakulin, A., Pittau, M. G., & Su, Y. S. (2008). A weakly informative default prior distribution for logistic and other regression models. *The Annals of Applied Statistics*, *2*, 1360–1383. https://doi.org/10.1214/08-AOAS191

Harasti, D., Lee, K. A., Gallen, C., Hughes, J. M., & Stewart, J. (2015). Movements, home range and site fidelity of snapper (*Chrysophrys auratus*) within a temperate marine protected area. *PLoS ONE*, *10*, e0142454. https://doi.org/10.1371/journal.pone.0142454

Hedger, R. D., Martin, F., Dodson, J. J., Hatin, D., Caron, F., & Whoriskey, F. G. (2008). The optimized interpolation of fish positions and speeds in an array of fixed acoustic receivers. *ICES Journal of Marine Science*, *65*, 1248–1259. https://doi.org/10.1093/icesjms/fsn109

Heupel, M. R., Semmens, J. M., & Hobday, A. J. (2006). Automated acoustic tracking of aquatic animals: Scales, design and deployment of listening station arrays. *Marine and Freshwater Research*, *57*, 1–13. https://doi.org/10.1071/MF05091

Hoffman, M. D., & Gelman, A. (2014). The No-U-turn sampler: Adaptively setting path lengths in Hamiltonian Monte Carlo. *Journal of Machine Learning Research*, *15*, 1593–1623.

Hussey, N. E., Hedges, K. J., Barkley, A. N., Treble, M. A., Peklova, I., Webber, D. M., … Fisk, A. T. (2017). Movements of a deep-water fish: Establishing marine fisheries management boundaries in coastal Arctic waters. *Ecological Applications*, *27*, 687–704. https://doi.org/10.1002/eap.1485

Huveneers, C., Simpfendorfer, C. A., Kim, S., Semmens, J. M., Hobday, A. J., Pederson, H., … Peddemors, V. (2016). The influence of environmental parameters on the performance and detection range of acoustic receivers. *Methods in Ecology and Evolution*, 7, 825–835. https://doi.org/10.1111/2041-210X.12520

Kessel, S. T., Cooke, S. J., Heupel, M. R., Hussey, N. E., Simpfendorfer, C. A., Vagle, S., & Fisk, A. T. (2014). A review of detection range testing in aquatic passive acoustic telemetry studies. *Reviews in Fish Biology and Fisheries*, 24, 199–218. https://doi.org/10.1007/s11160-013-9328-4

Kessel, S. T., Hussey, N. E., Webber, D. M., Gruber, S. H., Young, J. M., Smale, M. J., & Fisk, A. T. (2015). Close proximity detection interference with acoustic telemetry: The importance of considering tag power output in low ambient noise environments. *Animal Biotelemetry*, 3, 5. https://doi.org/10.1186/s40317-015-0023-1

Kneebone, J., Chisholm, J., Bernal, D., & Skomal, G. B. (2013). The physiological effects of capture stress, recovery, and post-release survivorship of juvenile sand tigers (*Carcharias taurus*) caught on rod and reel. *Fisheries Research*, 147, 103–114. https://doi.org/10.1016/j.fishres.2013.04.009

Kneebone, J., Chisholm, J., & Skomal, G. B. (2012). Seasonal residency, habitat use, and site fidelity of juvenile sand tiger sharks *Carcharias taurus* in a Massachusetts estuary. *Marine Ecology Progress Series*, 471, 165–181. https://doi.org/10.3354/meps09989

Kristensen, K., Nielsen, A., Berg, C. W., Skaug, H., & Bell, B. M. (2016). TMB: Automatic differentiation and Laplace approximation. *Journal of Statistical Software*, 70, 1–21. https://doi.org/10.18637/jss.v070.i05

Maunder, M. N., & Punt, A. E. (2013). A review of integrated analysis in fisheries stock assessment. *Fisheries Research*, 142, 61–74. https://doi.org/10.1016/j.fishres.2012.07.025

Payne, N. L., Gillanders, B. M., Webber, D. M., & Semmens, J. M. (2010). Interpreting diel activity patterns from acoustic telemetry: The need for controls. *Marine Ecology Progress Series*, 419, 295–301. https://doi.org/10.3354/meps08864

Pedersen, M. W., Burgess, G., & Weng, K. C. (2014). A quantitative approach to static sensor network design. *Methods in Ecology and Evolution*, 5, 1043–1051. https://doi.org/10.1111/2041-210X.12255

Pedersen, M. W., & Weng, K. C. (2013). Estimating individual animal movement from observation networks. *Methods in Ecology and Evolution*, 4, 920–929. https://doi.org/10.1111/2041-210X.12086

R Core Team. (2016). *R: A language and environment for statistical computing.* Vienna, Austria: R Foundation for Statistical Computing. Retrieved from https://www.R-project.org/

Royle, J. A., Chandler, R. B., Sollmann, R., & Gardner, B. (2014). *Spatial capture-recapture.* Waltham, MA: Academic Press.

Royle, J. A., & Dorazio, R. M. (2008). *Hierarchical modeling and inference in ecology: The analysis of data from populations, metapopulations and communities.* Boston, MA: Academic Press.

Simpfendorfer, C. A., Heupel, M. R., & Collins, A. B. (2008). Variation in the performance of acoustic receivers and its implication for positioning algorithms in a riverine setting. *Canadian Journal of Fisheries and Aquatic Sciences*, 65, 482–492. https://doi.org/10.1139/f07-180

Simpfendorfer, C. A., Heupel, M. R., & Hueter, R. E. (2002). Estimation of short-term centers of activity from an array of omnidirectional hydrophones and its use in studying animal movements. *Canadian Journal of Fisheries and Aquatic Sciences*, 59, 23–32. https://doi.org/10.1139/f01-191

Stan Development Team. (2017). RStan: the R interface to Stan. R package version 2.16.2. Retrieved from http://mc-stan.org

SUPPORTING INFORMATION

Additional supporting information may be found online in the Supporting Information section at the end of the article.

How to cite this article: Winton MV, Kneebone J, Zemeckis DR, Fay G. A spatial point process model to estimate individual centres of activity from passive acoustic telemetry data. *Methods Ecol Evol.* 2018;9:2262–2272. https://doi.org/10.1111/2041-210X.13080